Supplementary Information for:

Delays reducing waterborne and water-related infectious diseases in China under climate change

Maggie Hodges[1,2], Jessica H. Belle[1], Elizabeth J. Carlton[3], Song Liang[4], Huazhong Li[5], Wei Luo[6], Matthew C. Freeman[1], Yang Liu[1], Yang Gao[7], Jeremy J. Hess[1,2], Justin V. Remais[1*]

[1] Rollins School of Public Health, Emory University, Atlanta, GA, USA
[2] Emory University School of Medicine, Atlanta, GA, USA
[3] Colorado School of Public Health, University of Colorado, Denver, CO, USA
[4] College of Public Health and Health Professions, University of Florida, Gainesville, FL, USA
[5] Office of Disease Control and Emergency Response, China Center for Disease Control and Prevention, Beijing, PRC
[6] Research Center for Eco-Environmental Sciences, Chinese Academy of Sciences, Beijing, PRC
[7] Atmospheric Science and Global Change Division, Pacific Northwest National Laboratory, Richland, WA, USA

* Correspondence to: Dr. Justin V. Remais, Department of Environmental Health, Emory University; address: 1518 Clifton Road, Atlanta, Georgia, 30322; phone: 404-712-8908, fax: 404-727-8744; email: justin.remais@emory.edu

Supplementary Methods

Comparative risk assessment (CRA) methods were used to estimate the burden of disease attributable to shifts in temperature associated with climate change[1-3], using as a baseline previous estimates of the 2008 burden of disease attributable to unsafe WSH in China[4] derived from data sources detailed below. The analysis was carried out for 31 provincial level administrative districts within China, consisting of 22 provinces, 5 autonomous regions, and 4 municipalities. Projections of the burden of WSH-attributable disease were adjusted to account for population growth, urbanization, and changes in provincial age distribution. In order to account for uncertainty in both future climate conditions and future infrastructure development, we constructed 12 storylines (main manuscript text, Table 1) by combining output from four representative concentration pathways (RCPs)[5] and three projections of access to improved water and sanitation infrastructure, as we describe in detail the sections below.

To project the burden of WSH-attributable disease in China forward under climate change conditions at the provincial scale, we followed standard comparative risk assessment methods[1,3], carrying out the following analytical steps:

1. identification of climate sensitive health outcomes
2. quantitative estimation of the climate-health relationship
3. definition of exposure scenarios, and
4. estimation of the attributable burdens of disease

1. Identification of climate sensitive health outcomes and literature review

WSH-attributable disease was defined to include diseases resulting from consumption of contaminated water; poor personal, domestic, or agricultural hygiene associated with a lack of access to clean or adequate water; and direct contact with water-dwelling vectors or pathogens, as described previously[6]. A systematic literature review was conducted to identify studies quantifying the relationship between climate components and incidence of diarrheal diseases, malaria, dengue fever, and Japanese encephalitis, as well as STH and schistosomiasis prevalence. The literature review was performed across medical, environmental health, environmental science, and demographic journals using PubMed, EBSCO Host, and Google Scholar. In addition to examining prior reviews[2,7-9] for relevant publications, the search involved the following MeSH terms and keywords: 'climate change,' 'global warming,' 'temperature,' 'precipitation,' 'rainfall,' 'humidity,' 'health' and 'diarrhea,' 'malaria,' 'dengue,' 'Japanese encephalitis,' and 'risk.' Studies were selected for inclusion if they provided effect measures describing the relationship between temperature change and WSH-attributable disease incidence (diarrheal and vector-borne diseases) or prevalence (STH and schistosomiasis), allowing for the conversion of these effect measures to estimates of α, the change in rate ratios for a 1°C change in temperature. Only studies that provided their sample size and standard error were included in the analysis in order to support an aggregation of results using meta-analysis techniques. Manuscripts describing the relationship between climate variation and agent-specific diarrheal disease were excluded, given the many, varied etiologies of diarrheal disease and the inability to integrate the results of such studies into the current exposure-based analysis. The literature review provided the basis of the quantitative estimation of climate-health relationships described below.

While climate change will impact temperature, precipitation, relative humidity, and variability in these and other climate components, the limited availability of epidemiological studies accounting for variation in these three variables restricted the

current analysis to the response of disease incidence and prevalence to changes in temperature (°C). Studies pertaining to observed relationships between diarrheal disease incidence and discrete precipitation events[10-13], continuous precipitation[13,14], and relative humidity[15,16] were also discovered during the course of the literature review; however, due to the difficulty in developing estimates of the compounded impact of more than one climate variable on disease incidence, the analysis was restricted to the impact of temperature alone. Similarly, for helminthiases the review of the literature identified two review articles[17,18]; one article describing the relationship between schistosomiasis infection and modifiable environmental risk factors[19]; and one analysis carrying out predictive risk mapping to identify the probable distribution of schistosomiasis under altered climate conditions[20]. As these articles did not describe the relationship between climate variables and the incidence or prevalence of schistosomiasis and soil transmitted helminths, these diseases were excluded from the present analysis. Thus the analysis was restricted to the impact of temperature variation on diarrheal diseases, malaria, dengue fever, and Japanese encephalitis.

The results of the reviewed literature were used to estimate α, the proportional change in the rate ratio of each WSH-attributable disease associated with a 1°C increase in surface temperature. Because the risk of diarrheal diseases and the impact of climate on diarrheal diseases may vary depending on access to water and sanitation infrastructure, estimates were stratified by water and sanitation access scenarios. When multiple estimates were identified for a given disease and, in the case of diarrheal diseases, water and sanitation access scenarios, the results were aggregated using standard random effects meta-analysis methods[21]. The specific methods used for estimating changes in disease burden for each disease are described in detail below.

2. Quantitative estimation of climate-health relationships

Diarrheal diseases

Where prior estimates have assumed a limited impact of climate change on diarrheal disease in countries where the per capita GDP is greater than US$6,000 per year[1], studies in North America and Europe indicate that high-income countries are also susceptible to the effects of climate change on water and sanitation-attributable disease[12,22-24]. Therefore, our analysis did not include the impact of changing GDP on WSH-attributable disease, focusing instead on the potential impact that urbanization, changing demographic structure, and varying rates of access to improved water and sanitation would have on our outcome.

Because the impact of increases in temperature on diarrheal disease may vary depending on WSH access, each published α estimate for diarrheal diseases was matched to a water

and sanitation access scenarios based on the locations in which the research was conducted (see Supplementary Table 1). We classified studies into water and sanitation access scenarios typically found in China as described in our previous work[4]. While earlier work by Pruss and colleagues (2002) described six water and sanitation access scenarios, they noted that scenarios I and III do not occur on a large scale, and are therefore negligible in larger scale analyses[6]. Our 2008 analysis provided China-specific rate ratios (RRs) for WSH-attributable disease stratified by water and sanitation access scenario for scenarios II, IV, Va, Vb, and VI[4]. Due to the limited number of available studies identified by our review of the literature quantifying the climate sensitivity of diarrheal disease, as well as limited data on the water and sanitation access of the study populations in reviewed literature, we were unable to confidently distinguish between studies fitting scenario Va versus scenario Vb. Thus, we used the more conservative (smaller) baseline RR of the two scenarios, as determined by the China-specific literature review described previously[4], and grouped the populations of scenarios Va and Vb into 'Scenario V' for the remainder of the present analysis. Due to the challenges of matching studies to water and sanitation access scenarios and the small number of available studies used to estimate α values within each water and sanitation access scenario, a parallel analysis was carried out using a single, aggregate α value obtained by combining all effect measures identified in the literature review[21].

The α estimates were used to adjust scenario-specific RRs of diarrheal diseases attributable to unsafe water and sanitation determined by our 2008 analysis (termed '$RR_{baseline}$'; see equation 1.1)[4]. The result was an adjusted rate ratio ($RR_{adjusted}$) describing the RR of diarrheal diseases associated with exposure to the projected change in temperature (ΔT, °C; see *Definition of climate exposure scenarios*), within a specific province, ρ, for a population in a given water and sanitation access scenario, σ:

$$RR_{adjusted,\rho,\sigma} = RR_{baseline,\sigma}(1 + \alpha_{\sigma}\Delta T_{\rho}) \qquad (1.1)$$

The total population in each province was allocated proportionally into water and sanitation access scenarios (σ) based on each of the three development paths used to project changes in water and sanitation access and changing demographics (see *Estimation of the climate change attributable burden of disease*, below). As described in our prior work[4], we assumed all urban populations had water and sanitation access corresponding with scenario II (main text Table 2). The $RR_{adjusted,\rho,\sigma}$ values (equation 1.1) were combined with the proportion of the provincial population experiencing each scenario (F_{σ}) to calculate the population-weighted, WSH-attributable adjusted rate ratio of diarrheal diseases for the province (ρ) under climate change conditions

(equation 1.2). To estimate the projected incidence rate of diarrheal diseases ($IR_{projected,\rho,\sigma}$), each province's population-weighted $RR_{adjusted,\rho,\sigma}$ was then applied to the baseline IR ($IR_{baseline,\rho}$; equation 1.2), which was estimated for 2020 and 2030 using projected province-specific age distributions[25] and the rate of diarrheal diseases observed in established market economies[4,26].

$$IR_{projected,\rho,\sigma} = IR_{baseline,\rho} \sum_{\sigma} F_{\sigma} \left(RR_{adjusted,\rho,\sigma} - 1 \right) \quad (1.2)$$

The $IR_{projected,\rho,\sigma}$ of WSH-attributable diarrheal diseases was calculated for each province in 2020 and 2030, and age- and sex-specific estimates of incidence and mortality were estimated (see *Estimation of the climate change attributable burden of disease*, below). China-wide incidence and mortality rates were drawn from our previous work[4].

Vector-borne disease

Similar to equation 1.1, we used estimates of α extracted from the literature review to estimate an adjusted incidence rate ($IR_{adjusted}$) expressing the incidence of either malaria, dengue fever, or Japanese encephalitis associated with exposure to the projected change in temperature (ΔT, °C; see *Definition of climate exposure scenarios*) for the population in a specific province, ρ:

$$IR_{adjusted,\,\rho} = IR_{baseline,\,\rho}(1 + \alpha \Delta T_{\rho}) \quad (1.3)$$

The baseline WSH-attributable incidence rates of malaria, dengue fever, and Japanese encephalitis in 2020 and 2030 were calculated using projected population[25,27] and age distributions[25] for each province (see *Estimation of the climate change attributable burden of disease*, below), while assuming that the province- and age-specific incidence rates of WSH-attributable vector-borne disease from our prior work were held constant[4]. The analysis did not account for vector range expansion or contraction, and instead simply considered the climate change attributable change in incidence anticipated in the provinces and age categories where malaria, dengue fever, and Japanese encephalitis are currently observed.

3. Definition of climate exposure scenarios

Climate exposure scenarios accounted for changing temperatures associated with climate change and simultaneous shifts in China's total and regional populations. The years 2020 and 2030 were chosen as time horizons for our analysis in order to provide estimates that could be used to inform the upcoming 13th Five-Year Plan for China, as well as subsequent development planning. We chose to focus on shifts in temperature

due to the difficulty in developing estimates of the compounded impact of more than one climate variable on disease incidence.

Monthly temperature projections generated by the HadGEM2-ES (1.25° latitude x 1.875° longitude) global climate model[28] were obtained from the CMIP5 database[29]. Output was acquired for model runs representing the four RCPs used by the Intergovernmental Panel on Climate Change (IPCC) in the fifth assessment report (RCP 2.6, RCP 4.5, RCP 6.0, and RCP 8.5)[5,28]. These RCP scenarios were developed for use in climate simulation to provide information on possible development trajectories and their impact on major greenhouse gases, in a fashion comparable to the previously used Special Report on Emissions Scenarios (SRES) scenarios[5,30]. RCP 2.6 is consistent with a scenario describing stringent climate policies to limit greenhouse gas emissions, leading to a very low radiative forcing level, while RCPs 4.5 and 6.0 describe moderate stabilization of greenhouse gas emissions. RCP 8.5 is consistent with a very high baseline greenhouse gas emission scenario with high population growth and lower incomes in developing countries[5].

Depending on the subject of study, reference climates can be defined using relatively short (e.g., 3-8 year[31-33]) or long (e.g., 20-30 year[34-36]) periods. In this study, human health impacts of near-term changes in climate were evaluated in order to facilitate policy-making in China, and thus a short reference period was selected—centered on the year (2008) for which baseline estimates of disease were available[4]—and used to examine proximate impacts in 2020 and 2030. The reference climate was calculated by averaging the model-specific monthly temperatures for 2006 through 2010 to produce semi-decadal mean temperature values for each month of the year, centered around 2008. For each RCP, the projected monthly temperatures in 2018, 2019, 2020, 2021, and 2022 were subtracted from these 2008 semi-decadal mean monthly temperatures in each grid cell (1.25° latitude x 1.875° longitude), and the resulting temperature differences were then averaged both temporally and spatially, over the 5-year period and across each province, to produce the semi-decadal mean monthly surface temperature deviation from the 2008 reference climate in each province, ρ ($Td_{\rho,2020}$, °C; equation 2.1). An evaluation was carried out using 53 members of 33 CMIP5 models to assess the degree to which the five-year reference period was representative of the entire decade, and to evaluate how results of a health model based on the HadGEM2-ES member r2i1p1 used here may differ from those based on other CMIP5 models/members (see Supplementary Results). The spatially averaged difference between the 2008 mean monthly surface temperature and the semi-decadal mean monthly surface temperature projected in 2020 and 2030, $Td_{\rho,20X0}$, was calculated as:

$$\Sigma[T_n(a_n/A)] = \mathrm{Td}_{\rho,20\mathrm{X}0} \quad (2.1)$$

where T_n is the difference between the 2008 semi-decadal mean monthly surface temperature and the projected semi-decadal mean monthly surface temperature in grid cell n in the years 2020 or 2030 (where X=2 or X=3, respectively); a_n is the surface area of a population grid cell n; A is the surface area of the province ρ, and the summation is taken over the n population grid cells that fall within the boundaries of province ρ. $\mathrm{Td}_{\rho,2030}$ was calculated in an analogous fashion. The $\mathrm{Td}_{\rho,2020}$ and $\mathrm{Td}_{\rho,2030}$ values thus represent the spatially averaged differences between the 2008 semi-decadal mean monthly surface temperature and the semi-decadal mean monthly surface temperatures projected for 2020 and 2030, respectively, across all grid cells.

To account for the uneven distribution of population across provinces, a population-weighted exposure to changing temperature, $\Delta\mathrm{T}_\rho$ (°C), was calculated for each province, ρ. In brief, to calculate $\Delta\mathrm{T}_\rho$ each population grid cell (1.0 x 1.0 km) was assigned the projected temperature change of the overlying climate grid cell (1.25° lat x 1.875° long; approximately 100km x 200km) using ArcGIS 10.1 (ESRI, 2012). The temperature change in each grid cell was then multiplied by the proportion of the provincial population inhabiting that cell, and these values were summed across all population grid cells to generate $\Delta\mathrm{T}_{\rho,20\mathrm{X}0}$ in each province, ρ (equation 2.2):

$$\sum [T_n\,(p_n/P)] = \Delta\mathrm{T}_{\rho,\,20\mathrm{X}0} \quad (2.2)$$

where T_n is the difference between the 2008 semi-decadal mean monthly surface temperature and the projected semi-decadal mean monthly surface temperature in grid cell n in the years 2020 or 2030 (where X=2 or X=3, respectively); p_n is the population inhabiting grid cell n in the year 20X0; and P is the total population of province ρ in the year 20X0. The spatially averaged (Td_ρ), and the spatially averaged and population-weighted ($\Delta\mathrm{T}_\rho$) semi-decadal mean monthly temperature deviations from the 2008 reference climate were calculated in 2020 based on output from each of the four RCP scenarios, and this process was repeated for the years surrounding 2030 (Supplementary Tables 2 and 3). The resulting 2020 and 2030 $\Delta\mathrm{T}_\rho$ values were used to obtain province-specific $RR_{adjusted,\rho,\sigma}$ and $IR_{adjusted,\rho}$ values (equations 1.1 and 1.3) for diarrheal diseases and vector-borne disease.

4. Estimation of the climate change attributable burden of disease

Baseline health and infrastructure data and data sources

Estimates of baseline disease rates and water and sanitation access were drawn from our previous work describing the burden of disease attributable to unsafe water and sanitation in China in 2008[4] and adjusted for population growth, urbanization and

water and sanitation infrastructure development. Vector-borne disease incidence was derived from China's national infectious disease reporting system (NIDR) and diarrheal disease incidence was estimated from an exposure based analysis using methods described elsewhere[4,6]. Baseline incidence rates of these WSH-attributable diseases from our previous work[4] were adjusted for changes in population growth[25,27] and provincial age distribution[25] before being used as baseline IRs ($IR_{baseline,p}$; equations 1.2 and 1.3) in the current analysis. Baseline province specific estimates of access to each water and sanitation access scenario from our previous work[4] were adjusted for urbanization and for changes in access to improved water and sanitation infrastructure according to the three development paths described below.

Projection of demographic changes

Gridded population density projections (1km x 1km) for 2000 were obtained from the National Aeronautics and Space Administration's Socio-Economic Data and Applications Center (SEDAC)[37] and projected forward using the province specific growth and urbanization rates obtained for 2020 and 2030[25,27]. These sources were chosen in order to produce results most consistent with the midline UN projections for total and urban population for all of China[38]. While the sex-ratio was held constant at the level obtained from 2000 census data[4], the province-specific age distributions for 2030 were provided by projections made by Toth et al. (2003)[25]. Province-specific age distributions for 2020 were not available at the time of this analysis, and thus the 2020 province-specific age distributions were taken from predictions for 2015[25]; however, the province-specific age distributions projected by Toth (2003) for 2015[25] result in a country-wide age distribution that matches the UN midline predictions for China in 2020 to within three percentage points[38].

China's population growth and rapid rates of urbanization and internal migration were thus accounted for using projections of the overall urban proportion of each provincial population for 2020 and 2030 that incorporated province-specific estimates of internal migration and urbanization[25,27]. The resulting population distributions were summed across each province to generate total projected provincial populations in 2020 and 2030; these were compared and found to be in agreement with United Nations midline population projections[38] by a margin of 3.8% in 2020 and 2.4% in 2030. The projected provincial populations are presented in Supplementary Tables 2 and 3.

Projection of changes in WSH access

Since 1990, rapid improvements in access to water in China have been driven by both urbanization of the population and improved access in rural areas[39]. At the same time, improved access to sanitation has been dramatic. Yet, while there is now nearly

universal access in urban areas, coverage in rural areas is only 70%[39]. Guided by our previous work, we have defined improved water as including water from centralized, piped, regularly treated sources, and we have defined improved sanitation as sanitation systems able to isolate fecal waste (including sewer connections, triple compartment septic tanks, anaerobic biogas digesters, double barrel funnel type septic tanks, and urine-separating toilets with a septic tank)[4]. To examine the sensitivity of our results to assumptions regarding the rate of improvement in water and sanitation access, the WSH-attributable incidence of disease in 2020 and 2030 was estimated assuming three water and sanitation access development paths (depicted in Supplementary Figure 1): (1) maintenance level, where the *proportion* of the population in each province with access to improved water and sanitation infrastructure is unchanged from the levels reported for the baseline year (2008)[4]; (2) a linear rate of increase in the proportion of the population with access to improved water and sanitation infrastructure, generated by fitting a simple linear model to the data reported by the WHO and UNICEF Joint Monitoring Program for Water Supply and Sanitation (JMP) for the years 1990-2012[39], and projecting that model forward to 2020 and 2030 (this path is considered our 'midline estimate,' as it makes minimal assumptions about the future trend in infrastructure improvement in China beyond the trend observed from 1990 to 2012[39]); and (3) an exponential rate of increase in the proportion of the population with access to improved water and sanitation generated by fitting a simple exponential model to the JMP data reported for the years 1990-2012[39], and projecting that model forward to 2020 and 2030. These three water and sanitation access development paths represent increasingly ambitious policy options for China, and they were incorporated into twelve storylines (detailed in main text Table 1) for which the development delay attributable to climate change was estimated.

The demographic estimates of the overall urban proportion of each provincial population for 2020 and 2030 were used to define the proportion of the population experiencing the urban water and sanitation access scenario (scenario II). The projected rural proportion of the provincial populations were then assigned into the remaining water and sanitation access scenarios according to the three water and sanitation development paths, following the method used to define the baseline distributions reported in our earlier work[4].

Estimating attributable burden and development delays

The overall burden of WSH-attributable disease (in DALYs per 1,000 population) was calculated for each province under each of twelve storylines for 2020 and 2030 (main text Table 1) using non-uniform age-weighting, 3% discounting, and age and sex specific incidence and mortality counts. Disability weights, and disease durations were drawn

from established sources[4,40] to facilitate comparisons. Each storyline was defined by a combination of one of the four RCP scenarios and one of three development paths for access to improved water and sanitation infrastructure. The burden of WSH-attributable disease projected under each storyline was then compared to the burden of disease anticipated in 2020 and 2030 without the impact of climate change ('reference' storylines).

In order to summarize the impact of climate change on China's ongoing progress toward reducing WSH-attributable disease, a development delay, δ, at 2020 and 2030 was calculated for each province. The development delay expresses the additional time (in months) that a province would be required to continue to provide infrastructure improvement, health investments and other efforts in order to attain the burden of WSH-attributable disease predicted under a scenario without the impact of climate change (see Figure 1 in the main manuscript). The delay, δ, was then calculated as:

$$\delta = (B_{adjusted} - B_{reference}) / m \quad (3.1)$$

where the burden of disease in 2020 or 2030 is expressed as a proportion of the 2008 burden of disease, both with ($B_{adjusted}$) and without ($B_{reference}$) the impact of climate change; and m is the monthly rate of change in the burden of WSH-attributable disease over the time period evaluated for each storyline.

Sensitivity and uncertainty analyses

Sensitivity analyses were carried out to examine the impact of stratified versus combined α estimates for diarrheal diseases. WSH-attributable incidence of diarrheal diseases was estimated by replacing the α values stratified by water and sanitation access scenario with a single, aggregate α obtained by aggregating all effect measures (α values) identified through the review of literature on diarrheal diseases and climate. In addition, the 95% confidence intervals of α values identified during the literature review were propagated through the analysis using standard, random effects meta-analysis techniques[21] in order to quantify the impact of the uncertainty in the parent studies on our final results.

Supplementary Results

Results of literature review and quantitative estimation of climate-health relationships

The results of the literature review and meta-analysis are presented in Supplementary Table 1, and are described for each disease below.

Diarrheal disease. Perhaps the most well-known of these studies, Checkley (2000) observed the daily number of children under the age of 10-years old admitted to a Peruvian hospital with diarrhea before, during, and after an El Niño event and

described an increase in diarrheal disease incidence of 8% for each 1°C increase in mean ambient temperature (relative risk 1.08; 95% CI 1.07, 1.09)[15]. For patients over the age of 13-years old in Lima, Peru, Lama (2004) described a similar increase in the monthly incidence of diarrheal disease of 8.1% (95% CI 2.5, 14.1) for every 1°C increase in mean monthly temperature[41]. In Dhaka, Bangladesh, Hashizume (2007) described a 5.6% increase in the number of weekly, non-cholera diarrheal cases for every 1°C increase in mean weekly temperature (95%CI 3.4, 7.8)[13]. Focusing on the impact of temperature on bacillary dysentery incidence in Jinan, China, Zhang and colleagues (2008) described an 11.4% increase in incidence for every 1°C increase in maximum ambient temperature (95% CI 10.19, 12.69)[42]; however this study was excluded due to its focus on a single etiology of diarrheal disease. Singh and colleagues (2001) observed a 3.0% increase in the incidence of diarrhea among infants in Fiji for every 1°C increase in mean monthly temperature, on a one-month lag (95%CI 1.2, 5.0)[14]. Finally, Onozuka (2010) described a 7.7% increase in the incidence of infectious gastroenteritis cases with every 1°C increase in weekly mean temperature (95%CI 4.6, 10.8), observed in over 120 institutions across Fukuoka, Japan[16]. These studies were stratified by the water and sanitation access of their respective study populations, and assigned to the water and sanitation access scenarios described previously[4,6].

Malaria. Zhang and colleagues (2010) described the results of a 20-year time-series analysis of the incidence of malaria in Jinan, China; the results of two SARIMA regression models demonstrated a 10.2% (95%CI 7.7, 12.7) increase in malaria incidence for every 1°C increase in minimum temperature or a 13.8% (95%CI 11.8, 15.8) increase in malaria incidence for every 1°C increase in maximum temperature[43]. A time-series analysis of climate variables and malaria incidence in Yunnan, China demonstrated a 4.7% (95%CI 4.5, 5.0) increase in malaria incidence for every 1°C increase in mean monthly temperature[44]. Most recently, an analysis of civilian malaria cases from the Republic of Korea described a 16.1% (95%CI 15.3, 16.9) increase in malaria incidence for every 1°C increase in un-lagged mean weekly temperature, with the effect intensifying to a 17.7% (95% CI 16.9, 18.6) increase in malaria incidence for every 1°C increase in mean weekly temperature observed at a three week lag[45].

Dengue fever. Lu and colleagues (2009) described a risk ratio of 1.42 (95% CI 1.27, 1.57) associated with every 1°C increase in mean monthly temperature in Guangzhou City, China[46], while Pham (2011) observed a risk ratio of 1.21 (95%CI 1.10, 1.34) associated with every 2°C increase in mean monthly temperature in Dak Lak, Vietnam[47]. In addition to these studies, Chen (2010) observed a risk ratio of 1.15 associated with a 1°C increase mean weekly minimum temperature in Taipei, Taiwan, as well as a risk ratio of 1.705 associated with a 1°C increase mean weekly minimum temperature in

Kaohsiung, Taiwan[48], and Hi (2009) described a risk ratio of 1.23 associated with every 10°C increase mean weekly temperature in Singapore[49]. However, the studies by Chen (2010) and Hii (2009) provided neither confidence intervals nor standard errors for their effect measures and therefore could not be aggregated using the random effects meta-analysis technique utilized here[21].

Japanese encephalitis. One study by Bi (2007) performed in Jinyi City, China described a 7.9% (95% CI 3.3, 12.6) increase in the incidence of Japanese encephalitis for every 1°C increase in mean maximum monthly temperature[50]. A similar study by Bi (2003) in Jieshou City, China observed a 7.68% increase in incidence for every 1°C increase in mean maximum monthly temperature[51]; however this latter study failed to include confidence intervals or standard errors and was therefore excluded from the analysis.

Schistosomiasis and soil transmitted helminths. A review of the literature describing the climate sensitivity of schistosomiasis and STHs identified two review articles[17,18]; one article describing the relationship between schistosomiasis infection and modifiable risk factors[19]; and one analysis carrying out predictive risk mapping to identify the probable distribution of schistosomiasis under altered climate conditions[20]. These studies did not provide an estimate of α describing the relationship between climate variables and the incidence or prevalence of schistosomiasis nor soil transmitted helminths, and thus these diseases were excluded from the present analysis.

Anticipated climate change

The Fifth Assessment Report (AR5) of the IPCC projected 0.5-2.0°C of warming for China during the 2016-2035 time period[52] compared to the 1986-2005 baseline. China is warming approximately 0.22°C per decade[53], and thus the AR5 projection cited above, also developed using the four RCP scenarios, amounts to approximately 0.3-1.8°C of warming from 2008 to 2035, which is consistent with our estimated warming of 0.82 to 1.39°C during this time period[52]. By 2030, the population and GDP projections of RCP2.6, RCP4.5 and RCP6.0 do not differ from each other significantly. However, the 'Peak-Decline' pattern in radiative forcing experienced under RCP 2.6[5] yields a peak forcing level of 3.1 W/m^2 in the mid-21st century. Thus, we note that our projections have captured a timeframe where the projected Td (°C) for China is greater under RCP 2.6 than under RCPs 4.5 or 6.0 (see Supplementary Figure 4), before the projected decline in radiative forcing occurs[5]. The HadGEM2-ES member performed well against observed temperatures, and in fact outperformed most of the CMIP5 models (see below). Additionally, the 5-year periods used in this study exhibited no systematic biases when compared with 10-year periods (see below).

Assessing the representativeness of climate model and semi-decadal analysis

To evaluate whether HadGEM2-ES r2i1p1 (member 2) performed well in reproducing the climatological mean temperature, in Supplementary Figure 6 we compare HadGEM2-ES r2i1p1 (member 2), the HadGEM2-ES ensemble mean and a CMIP5 ensemble mean based on 33 CMIP5 models with a total of 53 members (Supplementary Table 5), with observational data (http://www.esrl.noaa.gov/psd/data/gridded/data.UDel_AirT_Precip.html). We also compared the bias of HadGEM2-ES with the ensemble mean of each CMIP5 model (Supplementary Figure 6). When compared to other CMIP5 models and members, HadGEM2-ES r2i1p1 (member 2) performed well against observed temperatures, and in fact outperformed most CMIP5 models (Supplementary Figure 6). The biases from HadGEM2-ES r2i1p1 (member 2), HadGEM2-ES ensemble mean and CMIP5 mean were comparable when both 5-year and 10-year periods were evaluated, although the models tend to underestimate the temperature in western China (Supplementary Figure 5). The 5-year periods used in this study exhibited no systematic biases when compared with 10-year periods (Supplementary Figure 5).

In order to further illustrate the degree to which the model used was representative of anticipated climate change, we compared the 5-year and 10-year mean changes of temperature from HadGEM2-ES r2i1p1 (member 2), HadGEM2-ES ensemble mean and CMIP5 mean for RCP 4.5 (Supplementary Figure 7) and RCP 8.5 (Supplementary Figure 8). HadGEM2-ES r2i1p1 (member 2) is generally consistent with CMIP5, with projected warming slightly stronger than the CMIP5 mean over parts of western China under RCP 4.5, and parts of eastern China under RCP 8.5.

Sensitivity analyses

We analyzed the sensitivity of the results to employing an aggregate α, as well as α values stratified by four water and sanitation access scenarios. As described briefly in the main text, compared with using the aggregate α, stratified values generally yielded slightly higher estimates for diarrheal disease burden. Estimates for 2020 ranged from 0.04% smaller to 1.19% larger and estimates for 2030 ranged from 0.44% smaller to 2.85% larger. Using stratified values made the smallest difference in estimates under storyline 3.1 (estimates using a stratified α are 0.04% smaller in 2020 and 0.14% smaller in 2030). Using stratified values yielded the largest difference for 2020 estimates under storyline 4.2, where estimates are 1.19% larger, and for 2030 estimates under storyline 4.3, where estimates are 2.85% larger.

Supplementary Table 1: Results of literature review regarding the sensitivity of WSH-disease to climate change.

Diarrheal disease	Location	Population	Wat/san scenario (α, 95% CI)	% Increase in incidence per 1°C increase in temp. (95% CI)	Variables in model	Duration of study	Source
	Fukuoka, Japan	All patients	II 0.077 (0.046, 0.108)	7.7 (4.6, 10.8)	Relative humidity, seasonality	1999-2007	Onozuka *et al,* 2010[16]
	Lima, Peru	<10yo	IV 0.08 (0.070, 0.090)	8 (7.0, 9.0)	Relative humidity	01/1/1993-11/15/1998	Checkley *et al,* 2000[15]
	Lima, Peru	Adults	IV 0.08 (0.070, 0.090)	8.1 (2.5, 14.1)	Presence of cholera cases, presence of weak or strong El Nino effect	1/1/1993-6/30/1998	Lama et al, 2004[41]
	Fiji	Infants	V 0.030 (0.012, 0.05)	3 (1.2, 5.0)	Rainfall, seasonality	1978-1989	Singh *et al,* 2001[14]
	Bangladesh	All patients	VI 0.056 (0.034, 0.078)	5.6 (3.4, 7.8)	Rainfall, seasonality	1/1996-12/2002	Hashizume *et al,* 2007[13]
Malaria	**Location**	**Population**	**% Increase in incidence per 1°C increase in temp. (95% CI)**		**Variables in model**	**Duration of study**	**Source**
	Jinan, China	All patients	10.2 (7.7, 12.7)		Seasonality, maximum temperature	1959-1979	Zhang *et al*, 2010[43]
	Jinan, China	All patients	13.8 (11.8, 15.8)		Seasonality, maximum temperature	1959-1979	Zhang et al, 2010[43]
	Yunnan, China	All patients	4.7 (4.5, 5.0)		Seasonality, monthly rainfall, provincial mean temporal trend	01/1991-12/2006	Clements *et al*, 2009[44]
	Republic of Korea	All civilian patients	17.7 (16.9, 18.6)		Seasonality, interannual variation, relative humidity, precipitation, DTR	2001-2009	Kim *et al*, 2012[45]
	Republic of Korea	All civilian patients	16.1 (15.3, 16.9)		Seasonality, interannual variation, relative humidity, precipitation, DTR	2001-2009	Kim *et al*, 2012[45]
Dengue fever	**Location**	**Population**	**% Increase in incidence per 1°C increase in temp. (95% CI)**		**Variables in model**	**Duration of study**	**Source**
	Guangzhou City, China	All patients	1.42 (1.27, 1.57)		Monthly minimum temp, monthly wind velocity, incidence of previous month	2001-2006	Lu *et al,*2009[46]
	Dak Lak, Vietnam	All patients	1.105 (1.05-1.17)		Household index, household mosquito, mean tem., rainfall	2004-2008	Pham *et al*, 2011[47]
Japanese encephalitis	**Location**	**Population**	**% Increase in incidence per 1°C increase in temp. (95% CI)**		**Variables in model**	**Duration of study**	**Source**
	Linyi City, China	All patients	7.9 (3.3, 12.6)		Mean max monthly temperature, mean monthly air pressure, monthly mean relative humidity, monthly total rainfall, year	1956-2004	Bi *et al*, 2007[50]

Supplementary Table 2: Estimated temperature deviation from 2008 baseline (Td_ρ, °C) by province and by RCP in 2020.

Province	2020 population (thousands)	RCP 2.6 Td_ρ	RCP 4.5 Td_ρ	RCP 6.0 Td_ρ	RCP 8.5 Td_ρ
Anhui	55,848	0.70	-0.07	0.46	1.06
Beijing	21,492	0.26	-0.06	0.09	1.32
Chonqing Shi	28,326	0.72	0.28	0.03	0.72
Fujian	36,732	0.65	0.10	0.40	0.98
Gansu	27,386	0.63	0.42	0.48	1.10
Guangdong	172,296	0.99	0.21	0.25	1.10
Guanxi	43,105	0.92	0.08	0.25	0.97
Guizhou	40,006	0.69	0.22	0.17	0.74
Hainan	9,500	1.00	0.21	-0.03	1.01
Hebei	75,419	0.26	-0.07	-0.35	1.20
Heilongjiang	35,296	-0.11	0.54	0.65	1.35
Henan	94,604	0.46	0.12	-0.09	1.28
Hubei	58,722	0.72	0.00	0.06	0.83
Hunan	55,761	0.81	0.03	0.15	0.85
Jaingsu	77,439	0.58	-0.05	0.49	1.28
Jiangxi	36,295	0.71	0.06	0.37	0.84
Jilin	25,212	-0.11	-0.40	0.64	1.37
Liaoning	39,762	0.23	-0.33	0.28	1.23
Neimenggu	24,438	0.03	0.08	0.09	1.49
Ningxia	7,006	0.42	0.35	0.03	0.97
Qinghai	5,630	0.83	0.60	-0.06	0.74
Shaanxi	38,823	0.48	0.31	-0.42	0.83
Shandong	91,447	0.41	-0.07	0.17	1.79
Shanghai	22,566	0.24	0.02	0.46	0.94
Shanxi	40,026	0.45	0.11	-0.61	0.90
Sichuan	72,247	0.90	0.54	0.17	0.58
Tianjin	12,034	0.32	-0.11	-0.02	1.34
Xinjiang	23,546	0.55	0.49	0.52	1.10
Xizang	2,938	0.93	0.65	0.34	0.64
Yunnan	52,390	1.03	0.56	0.30	0.42
Zhejiang	52,302	0.45	0.05	0.49	0.925
China	1,378,595	0.57	0.33	0.25	1.00

Supplementary Table 3: Estimated temperature deviation from 2008 baseline (Td_ρ, °C) by province and by RCP in 2030.

Province	2030 population (thousands)	RCP 2.6 Td_ρ	RCP 4.5 Td_ρ	RCP 6.0 Td_ρ	RCP 8.5 Td_ρ
Anhui	49,994	1.22	0.29	0.65	1.64
Beijing	24,710	0.75	-0.05	0.67	1.34
Chonqing Shi	32,540	1.18	0.72	0.62	1.19
Fujian	44,566	1.28	1.03	1.18	1.44
Gansu	30,813	1.15	0.55	0.96	1.52
Guangdong	180,129	1.41	1.16	1.25	1.59
Guanxi	39,300	1.37	0.94	1.31	1.58
Guizhou	34,628	1.25	0.87	1.02	1.27
Hainan	10,739	1.24	0.90	0.79	1.64
Hebei	74,319	0.69	0.00	0.32	1.39
Heilongjiang	31,077	-0.08	1.43	0.91	0.64
Henan	88,900	1.00	0.22	-0.30	1.94
Hubei	65,164	1.27	0.35	0.42	1.40
Hunan	56,894	1.38	0.62	0.85	1.53
Jaingsu	78,510	1.15	0.44	0.65	1.53
Jiangxi	41,011	1.42	0.74	1.08	1.58
Jilin	29,542	-0.09	1.07	0.72	0.72
Liaoning	40,951	0.36	0.70	0.61	0.91
Neimenggu	24,543	0.49	0.63	0.85	1.03
Ningxia	8,506	1.36	0.02	1.04	1.76
Qinghai	6,103	1.18	1.17	0.44	1.46
Shaanxi	35,123	1.14	0.35	0.06	1.44
Shandong	98,308	0.75	0.19	-0.26	2.05
Shanghai	28,308	0.97	0.40	0.87	1.31
Shanxi	41,435	1.01	-0.01	0.20	1.51
Sichuan	69,328	1.32	1.13	0.64	1.22
Tianjin	12,708	0.61	0.29	0.37	1.55
Xinjiang	26,606	1.11	0.59	1.36	1.78
Xizang	2,804	1.20	1.35	0.87	1.36
Yunnan	54,460	1.28	1.25	0.71	1.09
Zhejiang	57,125	1.10	0.83	1.06	1.49
China	1,419,143	0.99	0.82	0.83	1.39

Supplementary Table 4: Distribution of the total burden of WSH-attributable disease by scenario and disease etiology, using mean α values.

Storyline	Disease	2020		2030	
		Burden of disease (DALYs)	(% of total)	Burden of disease (DALYs)	(% of total)
0.1	Diarrhea	2,404,506	99.2	2,086,911	99.2
	Malaria	551	0.02	543	0.03
	Dengue fever	6	0.00024	6	0.00029
	Japanese encephalitis	19,255	0.79	16,225	0.77
0.2	Diarrhea	1,340,410	98.5	1,001,160	98.4
	Malaria	551	0.04	543	0.05
	Dengue fever	6	0.00042	6	0.00060
	Japanese encephalitis	19,255	1.42	16,225	1.59
0.3	Diarrhea	1,186,367	98.4	799,682	97.9
	Malaria	551	0.05	543	0.07
	Dengue fever	6	0.00048	6	0.00075
	Japanese encephalitis	19,255	1.60	16,225	1.99
1.1	Diarrhea	2,507,733	99.2	2,244,860	99.2
	Malaria	541	0.02	564	0.02
	Dengue fever	4	0.00017	6	0.00025
	Japanese encephalitis	19,061	0.75	17,145	0.76
1.2	Diarrhea	1,420,533	98.6	1,115,166	98.4
	Malaria	541	0.04	564	0.05
	Dengue fever	4	0.00030	6	0.00049
	Japanese encephalitis	19,061	1.32	17,145	1.51
1.3	Diarrhea	1,260,803	98.5	908,926	98.1
	Malaria	541	0.04	564	0.06
	Dengue fever	4	0.00034	6	0.00060
	Japanese encephalitis	19,061	1.49	17,145	1.85
2.1	Diarrhea	2,426,497	99.2	2,178,420	99.2
	Malaria	510	0.02	537	0.02
	Dengue fever	4	0.00015	5	0.00024
	Japanese encephalitis	18,329	0.75	16,538	0.75
2.2	Diarrhea	1,358,818	98.6	1,067,438	98.4
	Malaria	510	0.04	537	0.05
	Dengue fever	4	0.00027	5	0.00049
	Japanese encephalitis	18,329	1.33	16,538	1.52
2.3	Diarrhea	1,202,194	98.5	864,404	98.1
	Malaria	510	0.04	537	0.06
	Dengue fever	4	0.00030	5	0.00061
	Japanese encephalitis	18,329	1.50	16,538	1.88
3.1	Diarrhea	2,433,866	99.2	2,184,012	99.2
	Malaria	516	0.02	526	0.02
	Dengue fever	4	0.00015	5	0.00024
	Japanese encephalitis	18,301	0.75	16,480	0.75
3.2	Diarrhea	1,362,770	98.6	1,071,767	98.4
	Malaria	516	0.04	526	0.05
	Dengue fever	4	0.00027	5	0.00049
	Japanese encephalitis	18,301	1.32	16,480	1.51
3.3	Diarrhea	1,207,904	98.5	867,375	98.1
	Malaria	516	0.04	526	0.06
	Dengue fever	4	0.00030	5	0.00060
	Japanese encephalitis	18,301	1.49	16,480	1.86
4.1	Diarrhea	2,577,765	99.2	2,303,071	99.2
	Malaria	568	0.02	593	0.03
	Dengue fever	4	0.00017	6	0.00025
	Japanese encephalitis	19,247	0.74	17,410	0.75
4.2	Diarrhea	1,479,594	98.7	1,158,197	98.5
	Malaria	568	0.04	593	0.05
	Dengue fever	4	0.00029	6	0.00048
	Japanese encephalitis	19,247	1.28	17,410	1.48
4.3	Diarrhea	1,314,245	98.5	949,184	98.1
	Malaria	568	0.04	593	0.06
	Dengue fever	4	0.00032	6	0.00059
	Japanese encephalitis	19,247	1.44	17,410	1.80

Supplementary Table 5: CMIP5 models used in model validation/comparisons.

Model	Institution	NO. of members	Spatial Resolution (Lon×Lat, degree)
1. ACCESS1.0	Commonwealth Scientific and Industrial Research Organization (CSIRO), Australia and Bureau of Meteorology (BOM), Australia	1	1.875×1.25
2. ACCESS1.3		1	1.875×1.25
3. BCC-CSM1.1	Beijing Climate Center, China Meteorological Administration	1	2.81×2.77
4. BNU-ESM	Beijing Normal University, China	1	2.81×2.77
5. CanESM2	Canadian Centre for Climate Modelling and Analysis, Canada	1	2.81×2.79
6. CCSM4	National Center for Atmospheric Research, USA	6	1.25×0.9
7. CESM1-BGC	National Science Foundation, Department of Energy, NCAR, USA	1	1.25×0.9
8. CESM1-CAM5		3	1.25×0.9
9. CMCC-CM	Euro-Mediterraneo sui Cambiamenti Climatici, Italy	1	0.75×75
10. CMCC-CMS		1	1.875×1.86
11. CNRM-CM5	Centre National de Recherches Meteorologiques, Meteo-France, France	1	1.41×1.40
12. CSIRO-Mk3.6.0	Commonwealth Scientific and Industrial Research Organization (CSIRO), Australia	6	1.875×1.86
13. EC-EARTH	European Earth System Model	3	1.125×1.12
14. FGOALS_g2	Institute of Atmospheric Physics, Chinese Academy of Sciences, China	1	2.81×2.79
15. GFDL-ESM2M	NOAA Geophysical Fluid Dynamics Laboratory, USA	1	2.5×2.0
16. GFDL-ESM2G		1	2.5×2.0
17. GISS-E2-R	NASA Goddard Institute for Space Studies, USA	1	2.5×2.0
18. GISS-E2-H		1	2.5×2.0
19. HadGEM2_AO	Met Office Hadley Centre, UK	1	1.875×1.25
20. HadGEM2_CC		1	1.875×1.25
21. HadGEM2_ES		4	1.875×1.25
22. INM-CM4	Institute for Numerical Mathematics, Russia	1	2.0×1.5
23. IPSL-CM5A-LR	Institut Pierre-Simon Laplace, France	3	3.75×1.875
24. IPSL-CM5A-MR		1	2.5×1.25
25. IPSL-CM5B-LR		1	3.75×1.875
26. MIROC-ESM	Atmosphere and Ocean Research Institute (The University of Tokyo), National Institute for Environmental Studies and Japan Agency for Marine-Earth Science and Technology	1	2.81×1.77
27. MIROC-ESM-CHEM		1	2.81×1.77
28. MIROC5		2	1.41×1.39
29. MPI-ESM-LR	Max Planck Institute for Meteorology, Germany	1	1.875×1.85
30. MPI-ESM-MR		1	1.875×1.85
31. MRI-CGCM3	Meteorological Research Institute, Japan	1	1.125×1.125
32. NorESM1-M	Norwegian Climate Centre	1	2.5×1.875
33. NorESM1-ME		1	2.5×1.875

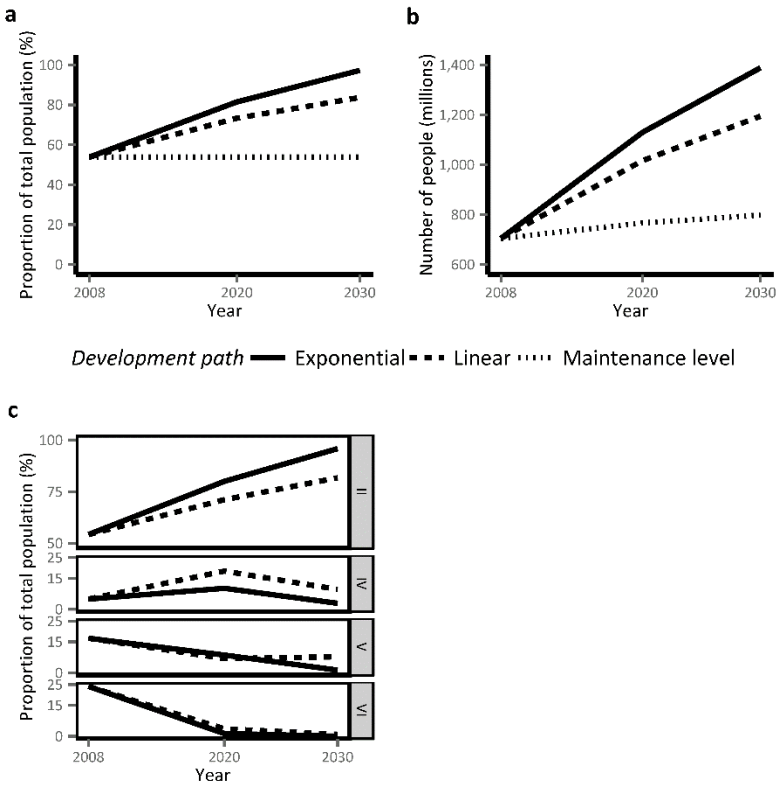

Supplementary Figure 1: Proportion of total (a) and number of people (b) with access to both improved water and sanitation (Scenario II) by development path. At bottom (c), the proportion of population in each Scenario (II, IV, V, VI) is shown for the exponential and linear development paths. See Table 2 in the main manuscript for scenario definitions.

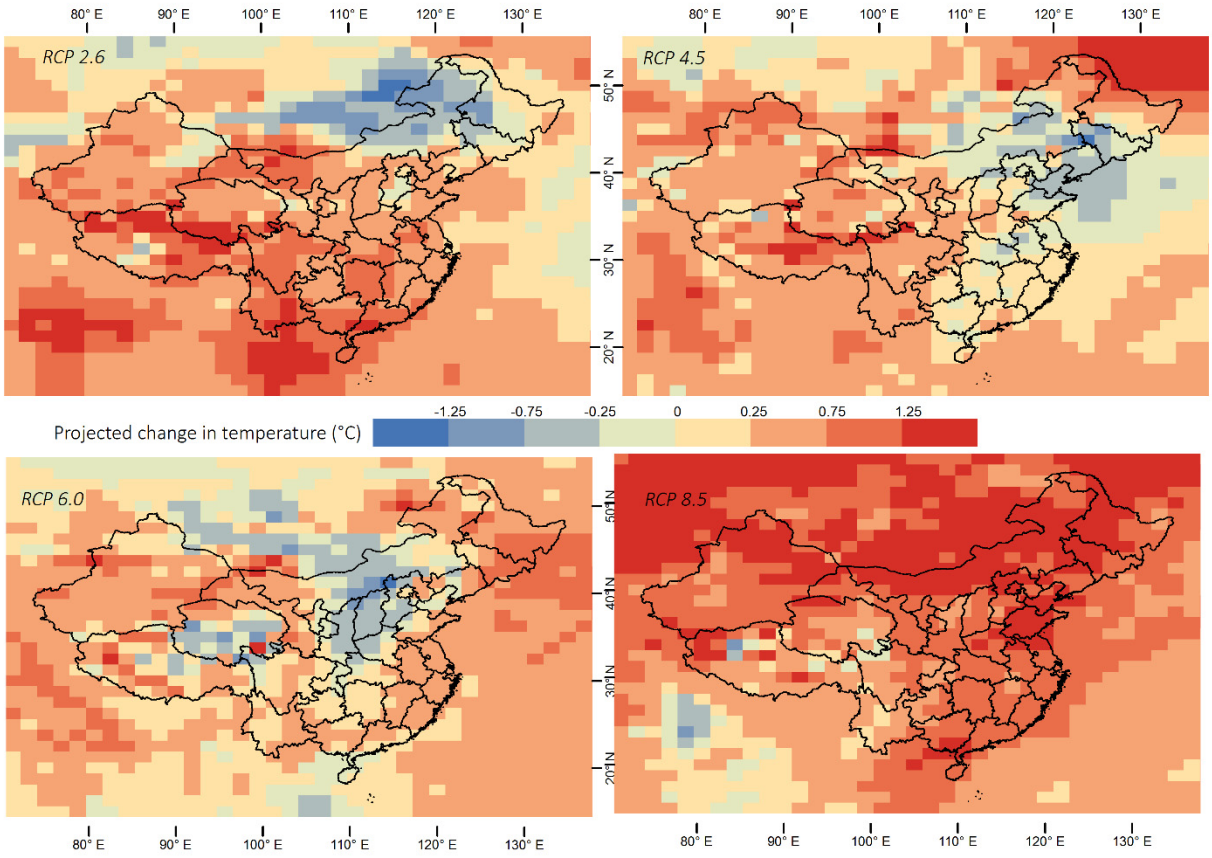

Supplementary Figure 2: Temperature deviations from reference climate to 2020, $Td_{\rho,2020}$.

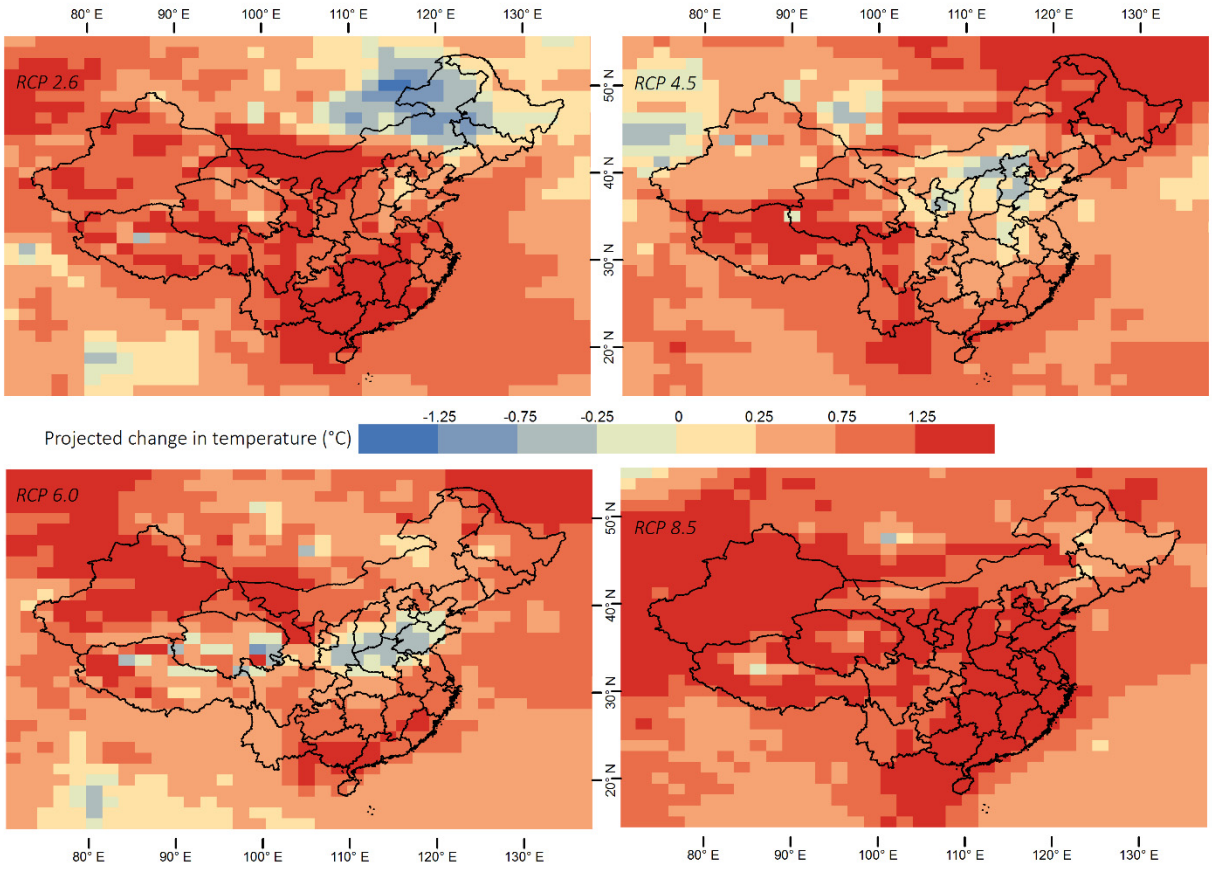

Supplementary Figure 3: Temperature deviations from reference climate to 2030, $Td_{\rho,2030}$.

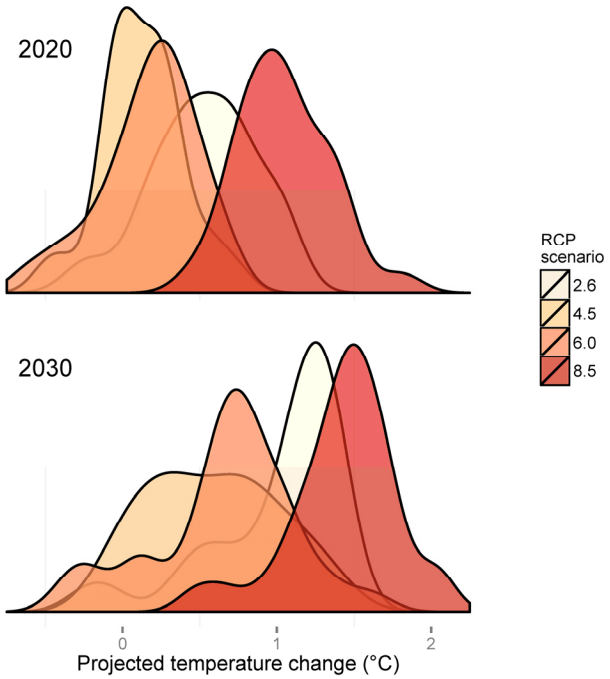

Supplementary Figure 4: Distribution of population-weighted provincial temperature deviations, ΔT_ρ, from 2008 under RCP 2.6, 4.5 6.0 and RCP 8.5. The y-axis represents the proportion of provinces across China experiencing a given ΔT_ρ value.

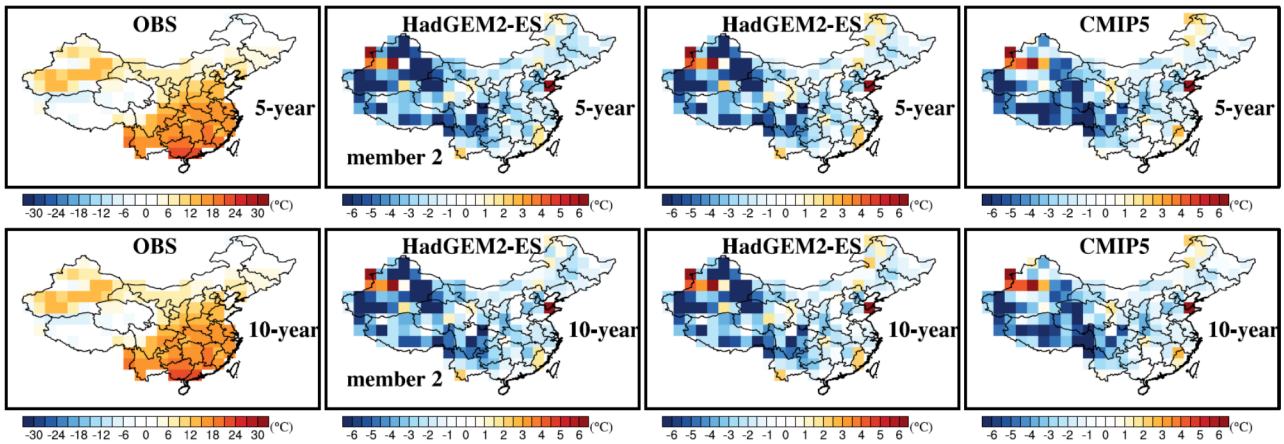

Supplementary Figure 5. Evaluation of 5-year and 10-year mean from HadGEM2-ES r2i1p1 (member 2), HadGEM2-ES ensemble mean and CMIP5 mean. The OBS shows the climatology mean in the 5-year (2006-2010) and 10-year (2001-2010) period, and the other panels display the biases (model results – OBS) for HadGEM2-ES r2i1p1 (member 2), HadGEM2-ES ensemble mean and CMIP5 mean. All models and observations have been interpolated to 2.5 by 2.5 degrees for ease of comparison.

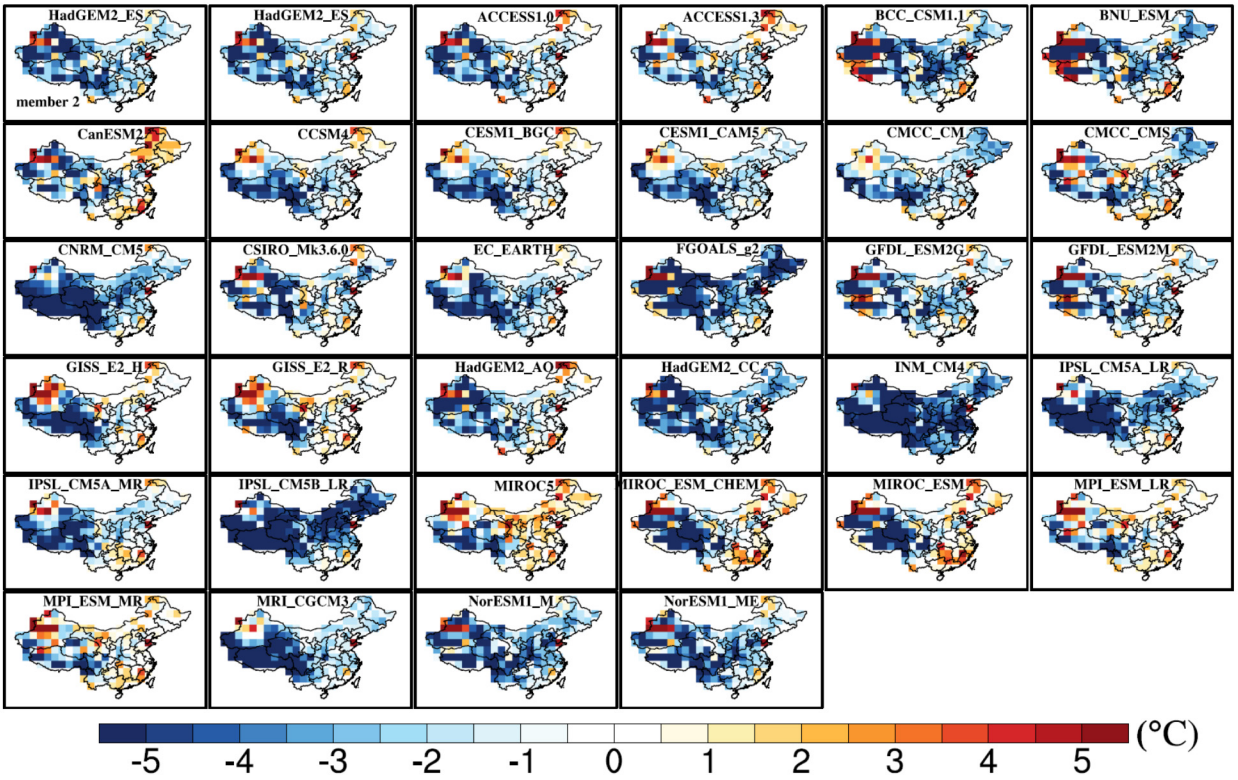

Supplementary Figure 6. The bias of HadGEM2-ES r2i1p1 (member 2), HadGEM2-ES ensemble mean and the other CMIP5 models using 10-year mean of observations from 2001-2010, calculated as model-OBS per Supplementary Figure 5.

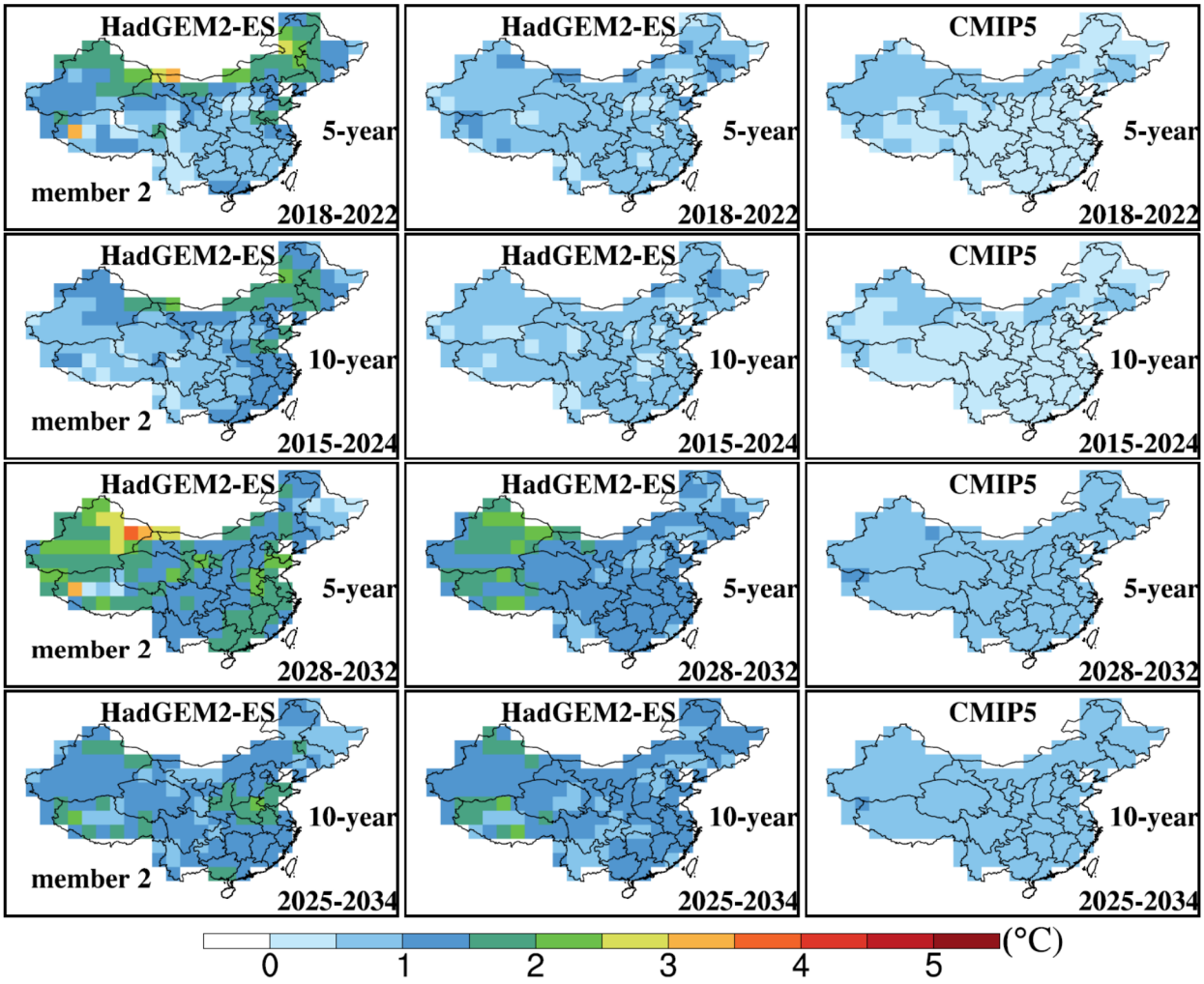

Supplementary Figure 7. Mean temperature deviations under RCP 4.5 from HadGEM2-ES r2i1p1 (member 2), HadGEM2-ES ensemble mean and the CMIP5 ensemble mean using 5-year and 10-year periods. The 5-year periods were referenced to 2006-2010; the 10-year periods were referenced to 2001-2010.

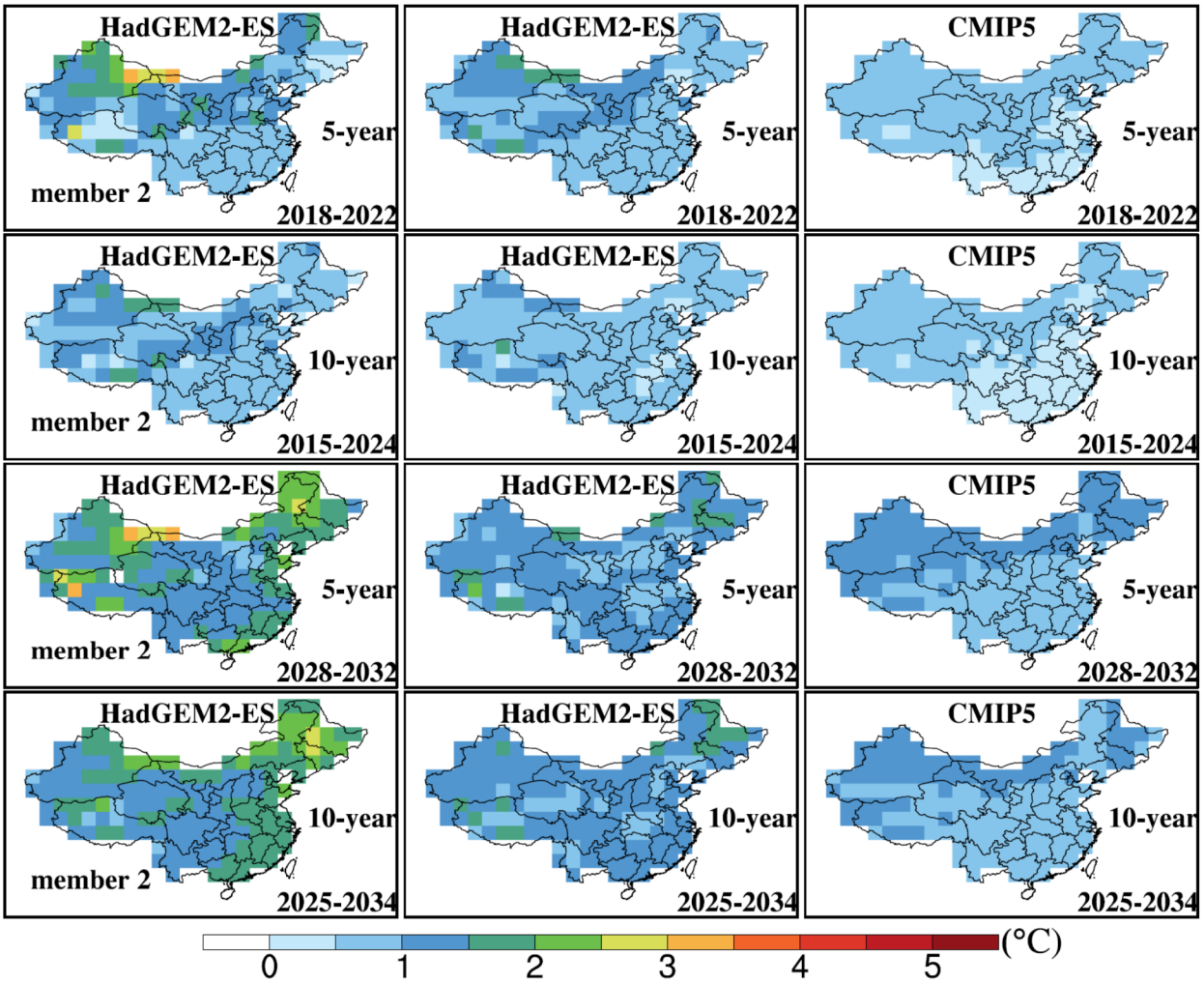

Supplementary Figure 8. Mean temperature deviations under RCP 8.5 from HadGEM2-ES r2i1p1 (member 2), HadGEM2-ES ensemble mean and the CMIP5 ensemble mean using 5-year and 10-year periods. The 5-year periods were referenced to 2006-2010; the 10-year periods were referenced to 2001-2010.

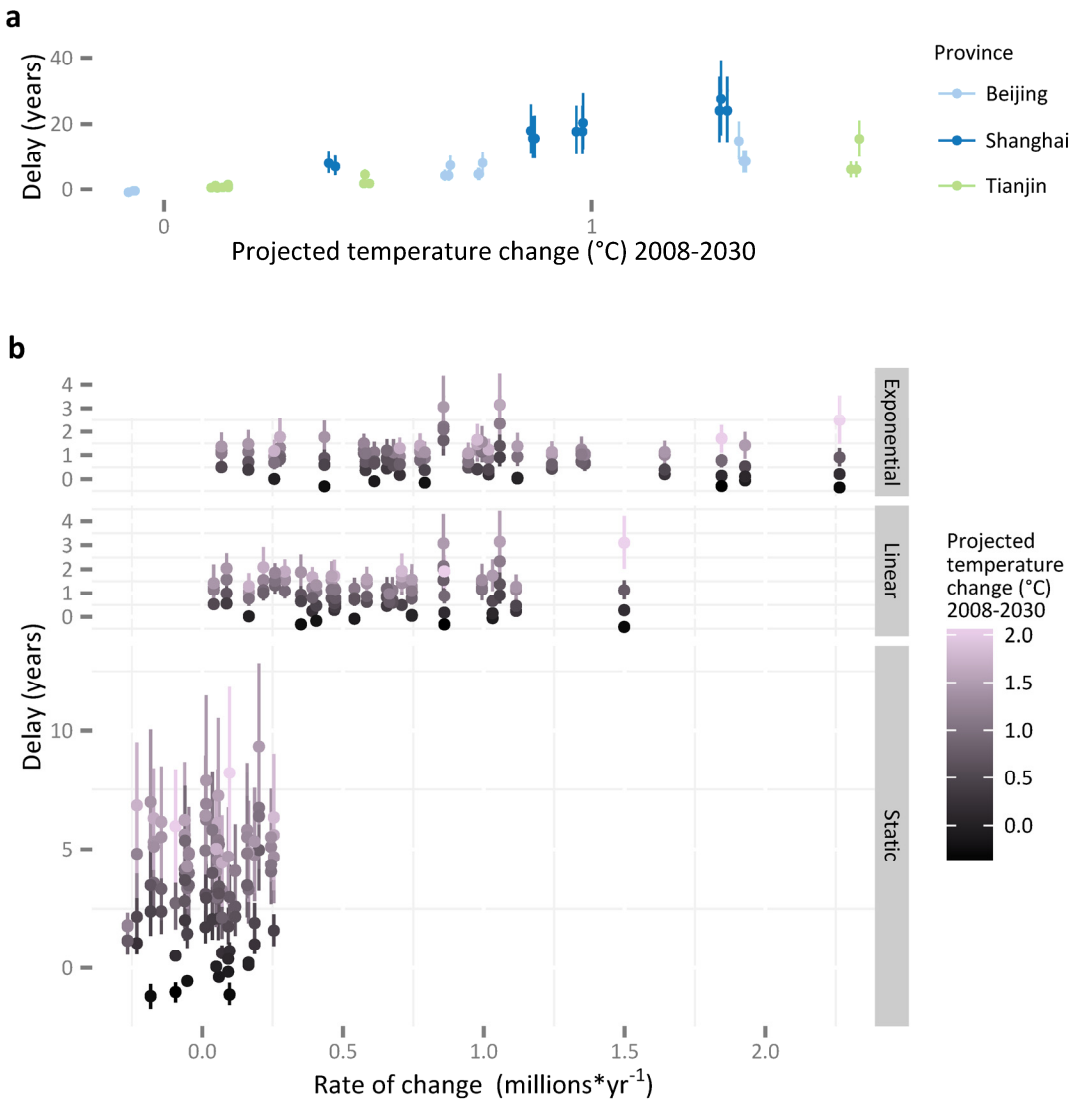

Supplementary Figure 9. Province-specific delay values in 2030 shown as a function of the rate of change in the number of people with water and sanitation access. Projected temperature change 2008-2030 is also indicated, as is the water and sanitation development path (panel b). Delays calculated for Shanghai, Beijing, Tianjin, and Guangdong are shown in top panel (a) in relation to projected temperature change.

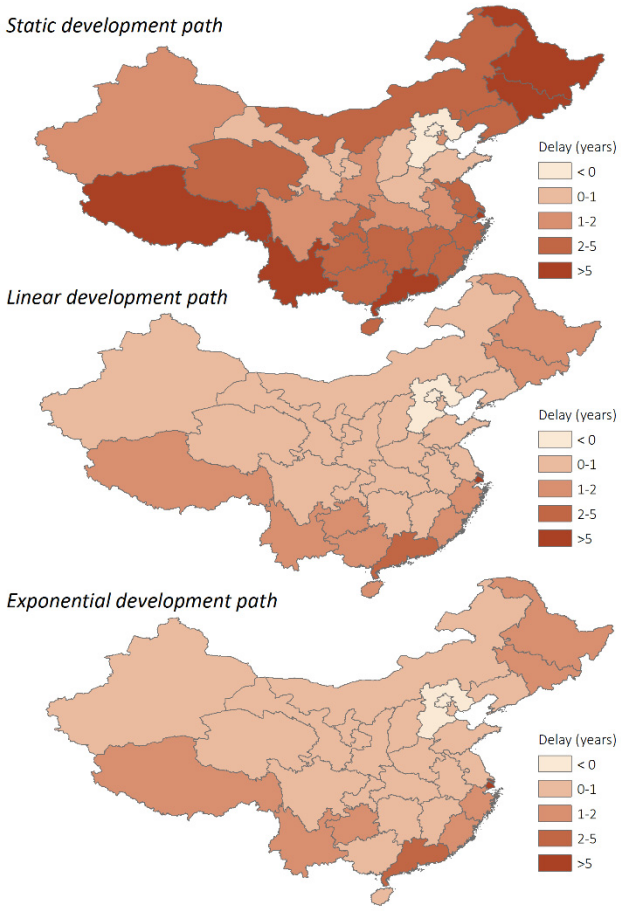

Supplementary Figure 10: Map of development delay values (in years) in 2030 under RCP 4.5.

Supplementary References

1 McMichael, A. J. *et al.* in *Comparitive Quantification of Health Risks: Global and Regional Burden of Disease Attributable to Selected Major Risk Factors* Vol. 1 (eds M. Ezzati, A. D. Lopez, A. Rodgers, & C.J.L. Murray) Ch. 20, 1543-1649 (World Health Organization, 2004).

2 Campbell-Lendrum, D. & Woodruff, R. Comparative risk assessment of the burden of disease from climate change. *Environ Health Perspect* **114**, 1935-1941 (2006).

3 Lim, S. S. *et al.* A comparative risk assessment of burden of disease and injury attributable to 67 risk factors and risk factor clusters in 21 regions, 1990-2010: a systematic analysis for the Global Burden of Disease Study 2010. *Lancet* **380**, 2224-2260, doi:10.1016/S0140-6736(12)61766-8 (2012).

4 Carlton, E. J. *et al.* Regional disparities in the burden of disease attributable to unsafe water and poor sanitation in China. *Bull World Health Organ* **90**, 578-587, doi:10.2471/BLT.11.098343 (2012).

5 Vuuren, D. P. *et al.* The representative concentration pathways: an overview. *Climatic Change* **109**, 5-31, doi:10.1007/s10584-011-0148-z (2011).

6 Pruss, A., Kay, D., Fewtrell, L. & Bartram, J. Estimating the burden of disease from water, sanitation, and hygiene at a global level. *Environmental Health Perspectives* **110**, 537-542 (2002).

7 Kolstad, E. W. & Johansson, K. A. Uncertainties associated with quantifying climate change impacts on human health: a case study for diarrhea. *Environ Health Perspect* **119**, 299-305, doi:10.1289/ehp.1002060 (2011).

8 Hunter, P. R. Climate change and waterborne and vector-borne disease. *J Appl Microbiol* **94 Suppl**, 37S-46S (2003).

9 McMichael, A. J., Woodruff, R. E. & Hales, S. Climate change and human health: present and future risks. *Lancet* **367**, 859-869, doi:Doi 10.1016/S0140-6736(06)68079-3 (2006).

10 Kondo, H. *et al.* Post-flood--infectious diseases in Mozambique. *Prehospital and disaster medicine* **17**, 126-133 (2002).

11 Thomas, K. M. *et al.* A role of high impact weather events in waterborne disease outbreaks in Canada, 1975 - 2001. *Int J Environ Health Res* **16**, 167-180, doi:10.1080/09603120600641326 (2006).

12 Drayna, P., McLellan, S. L., Simpson, P., Li, S. H. & Gorelick, M. H. Association between Rainfall and Pediatric Emergency Department Visits for Acute Gastrointestinal Illness. *Environmental Health Perspectives* **118**, 1439-1443, doi:Doi 10.1289/Ehp.0901671 (2010).

13 Hashizume, M. *et al.* Association between climate variability and hospital visits for non-cholera diarrhoea in Bangladesh: effects and vulnerable groups. *Int J Epidemiol* **36**, 1030-1037, doi:10.1093/ije/dym148 (2007).

14 Singh, R. B. *et al.* The influence of climate variation and change on diarrheal disease in the Pacific Islands. *Environ. Health Perspect.* **109**, 155-159 (2001).

15 Checkley, W. *et al.* Effects of El Nino and ambient temperature on hospital admissions for diarrhoeal diseases in Peruvian children. *Lancet* **355**, 442-450 (2000).

16 Onozuka, D., Hashizume, M. & Hagihara, A. Effects of weather variability on infectious gastroenteritis. *Epidemiol Infect* **138**, 236-243, doi:10.1017/S0950268809990574 (2010).

17 Weaver, H. J., Hawdon, J. M. & Hoberg, E. P. Soil-transmitted helminthiases: implications of climate change and human behavior. *Trends Parasitol* **26**, 574-581, doi:10.1016/j.pt.2010.06.009 (2010).

18 Mas-Coma, S., Valero, M. A. & Bargues, M. D. Climate change effects on trematodiases, with emphasis on zoonotic fascioliasis and schistosomiasis. *Veterinary Parasitology* **163**, 264-280, doi:DOI 10.1016/j.vetpar.2009.03.024 (2009).

19 Liang, S. *et al.* Environmental effects on parasitic disease transmission exemplified by schistosomiasis in western China. *Proc Natl Acad Sci U S A* **104**, 7110-7115, doi:DOI 10.1073/pnas.0701878104 (2007).

20 Zhou, X. N. *et al.* Potential impact of climate change on schistosomiasis transmission in China. *Am J Trop Med Hyg* **78**, 188-194, doi:78/2/188 [pii] (2008).

21 Borenstein, M., Hedges, L. V., Higgins, J. P. T. & Rothstein, H. R. A basic introduction to fixed-effect and random effects models for meta-analysis. *Research Synthesis Methods*, 97-111, doi:10.1002/jsrm.12 (2010).

22 Curriero, F. C., Patz, J., Rose, J. B. & Lele, S. The Association Between Extreme Precipitation and Waterborne Disease Outbreaks in the United States, 1948–1994. *Am J Public Health* **91**, 1194-1199 (2001).

23 Ahern, M., Kovats, R. S., Wilkinson, P., Few, R. & Matthies, F. Global health impacts of floods: epidemiologic evidence. *Epidemiol Rev* **27**, 36-46, doi:10.1093/epirev/mxi004 (2005).

24 Semenza, J. C. *et al.* Climate Change Impact Assessment of Food- and Waterborne Diseases. *Critical Reviews in Environmental Science and Technology* **42**, 857-890, doi:Doi 10.1080/10643389.2010.534706 (2012).

25 Toth, F., Cao, G. & Hizynyik, E. Regional population projections for China. Report No. IR-03-042, (International Institute for Applied Systems Analysis, 2003).

26 World Health Organization. The global burden of disease: 2004 update. (World Health Organization., Geneva, 2008).

27 Landoni, M. *Two scenarios on Chinese population dynamics based on a multiregional projection model*, Duke University, (2006).

28 Met Office Hadley Centre & Instituto Nacional de Pesquisas Espaciais. (U.S. Department of Energy Program for Climate Model Diagnosis and Intercomparison,, 2012).

29 Taylor, K. E., Stouffer, R. J. & Meehl, G. A. An Overview of CMIP5 and the Experiment Design. *Bulletin of the American Meteorological Society* **93**, 485-498, doi:10.1175/bams-d-11-00094.1 (2012).

30 Meehl, G. A. *et al.* Climate System Response to External Forcings and Climate Change Projections in CCSM4. *Journal of Climate* **25**, 3661-3683 (2012).

31 Gao, Y., Fu, J. S., Drake, J. B., Liu, Y. & Lamarque, J. F. Projected changes of extreme weather events in the eastern United States based on a high resolution climate modeling system. *Environmental Research Letters* **7** (2012).

32 Gao, Y., Fu, J. S., Drake, J. B., Lamarque, J. F. & Liu, Y. The impact of emission and climate change on ozone in the United States under representative concentration pathways (RCPs). *Atmospheric Chemistry and Physics* **13**, 9607-9621 (2013).

33 Ganguly, A. R. *et al.* Higher trends but larger uncertainty and geographic variability in 21st century temperature and heat waves. *Proc Natl Acad Sci U S A* **106**, 15555-15559, doi:10.1073/pnas.0904495106 (2009).

34 Hansen, J., Sato, M. & Ruedy, R. Perception of climate change. *Proc Natl Acad Sci U S A* **109**, E2415-2423, doi:10.1073/pnas.1205276109 (2012).

35 Sillmann, J., Kharin, V. V., Zhang, X., Zwiers, F. W. & Bronaugh, D. Climate extremes indices in the CMIP5 multimodel ensemble: Part 1. Model evaluation in the present climate. *Journal of Geophysical Research-Atmospheres* **118**, 1716-1733 (2013).

36 Gao, Y. *et al.* Robust spring drying in the southwestern U.S. and seasonal migration of wet/dry patterns in a warmer climate. *Geophysical Research Letters* **41**, 1745–1751 (2014).

37 CIESIN & CIAT. in *Gridded Population of the World* (CIESIN, Columbia University, Palisades, New York, 2011).

38 United Nations Population Division. *World Population Prospects, The 2010 Revision*, <http://www.un.org/esa/population/unpop.htm> (2010).

39 WHO/UNICEF Joint Monitoring Program. China: estimates on the use of water sources and sanitation facilities (1980-2012). (World Health Organization, 2014).

40 Murray, C. L. J. & Lopez, A. D. *The global burden of disease: a comprehensive assessment of mortality and disability from diseases, injuries, and risk factors in 1990 and projected to 2020.*, (Harvard University Press, 1996).

41 Lama, J. R., Seas, C. R., Leon-Barua, R., Gotuzzo, E. & Sack, R. B. Environmental temperature, cholera, and acute diarrhoea in adults in Lima, Peru. *J Health Popul Nutr* **22**, 399-403 (2004).

42 Zhang, Y., Bi, P. & Hiller, J. E. Weather and the transmission of bacillary dysentery in Jinan, northern China: a time-series analysis. *Public Health Rep* **123**, 61-66 (2008).

43 Zhang, Y., Bi, P. & Hiller, J. E. Meteorological variables and malaria in a Chinese temperate city: A twenty-year time-series data analysis. *Environ Int* **36**, 439-445, doi:10.1016/j.envint.2010.03.005 (2010).

44 Clements, A. C., Barnett, A. G., Cheng, Z. W., Snow, R. W. & Zhou, H. N. Space-time variation of malaria incidence in Yunnan province, China. *Malar J* **8**, 180, doi:10.1186/1475-2875-8-180 (2009).

45 Kim, Y. M., Park, J. W. & Cheong, H. K. Estimated Effect of Climatic Variables on the Transmission of Plasmodium vivax Malaria in the Republic of Korea. *Environ Health Perspect* **120**, 1314-1319, doi:10.1289/ehp.1104577 (2012).

46 Lu, L. *et al.* Time series analysis of dengue fever and weather in Guangzhou, China. *BMC Public Health* **9**, 395, doi:10.1186/1471-2458-9-395 (2009).

47 Pham, H. V., Doan, H. T., Phan, T. T. & Minh, N. N. Ecological factors associated with dengue fever in a Central Highlands province, Vietnam. *BMC Infect Dis* **11**, 172, doi:10.1186/1471-2334-11-172 (2011).

48 Chen, S. C. *et al.* Lagged temperature effect with mosquito transmission potential explains dengue variability in southern Taiwan: insights from a statistical analysis. *Sci Total Environ* **408**, 4069-4075, doi:10.1016/j.scitotenv.2010.05.021 (2010).

49 Hii, Y. L. *et al.* Climate variability and increase in intensity and magnitude of dengue incidence in Singapore. *Glob Health Action* **2**, doi:10.3402/gha.v2i0.2036 (2009).

50 Bi, P., Zhang, Y. & Parton, K. A. Weather variables and Japanese encephalitis in the metropolitan area of Jinan city, China. *J Infect* **55**, 551-556, doi:10.1016/j.jinf.2007.07.004 (2007).

51 Bi, P., Tong, S., Donald, K., Parton, K. A. & Ni, J. Climate variability and transmission of Japanese encephalitis in eastern China. *Vector Borne Zoonotic Dis* **3**, 111-115, doi:10.1089/153036603768395807 (2003).

52 IPCC. Climate Change 2013: The Physical Science Basis: Contribution of Working Group I to the Fifth Assessment Report of the Intergovernmental Panel on Climate Change. (Cambridge University Press, Cambridge, 2013).

53 Ding, Y. H. *et al.* Detection, causes and projection of climate change over China: An overview of recent progress. *Advances in Atmospheric Sciences* **24**, 954-971, doi:DOI 10.1007/s00376-007-0954-4 (2007).